J Radioanal Nucl Chem
DOI 10.1007/s10967-013-2561-4

Sedimentation and lateral transport of ^{210}Pb over the East China Sea Shelf

Ziming Fang · Weifeng Yang · Xinxing Zhang · Min Chen · Dejiang Fan · Qiang Ma · Run Zhang · Minfang Zheng · Yusheng Qiu

Received: 2 January 2013

Abstract ^{210}Pb is an effective tracer of constraining particle transport and sedimentation in shelf regions. To reveal the spatial pattern of ^{210}Pb over the East China Sea (i.e. ECS) Shelf, ^{210}Pb in the surface sediments were examined at 11 stations, as well as ^{234}Th and ^{210}Pb in the water column at four stations. Overall, the plume zone of the Yangtze River along the coastline is a source area of ^{210}Pb for the outer shelf, exporting 0.46 dpm cm^{-2} year^{-1} at least, which accounts for about 25 % of ^{210}Pb input into this region. In the southern ECS Shelf to the north of the Taiwan Strait, the focusing factor (f) values are higher than unity, indicating a sink area of ^{210}Pb. Boundary scavenging of ^{210}Pb contributes 0.36 dpm cm^{-2} year^{-1} to this sink area on the basis of a mass balance model evaluation. Lateral transport of ^{210}Pb to this region, quantified by ^{234}Th and ^{210}Pb in the water column, varied from 3.34 to 6.39 dpm cm^{-2} year^{-1} with an average of 4.83 dpm cm^{-2} year^{-1}, also supporting its sink characteristic. To the southwest of the Cheju Island, the f values were less than unity, revealing a source region of ^{210}Pb. The average export flux of ^{210}Pb from this region was 1.64 dpm cm^{-2} year^{-1}. Therefore, ^{210}Pb sedimentation/settling showed significantly heterogeneous sedimentation of particulate matter over the ECS Shelf.

Keywords ^{210}Pb · Boundary scavenging · ^{234}Th · East China Sea · Lateral transport

Z. Fang · W. Yang (✉) · X. Zhang · M. Chen · Q. Ma · R. Zhang · M. Zheng · Y. Qiu
State Key Laboratory of Marine Environmental Science, Xiamen University, Xiamen 361005, China
e-mail: wyang@xmu.edu.cn

D. Fan
College of Marine Geosciences, Ocean University of China, Qingdao 266003, China

Introduction

The East China Sea (ECS), situated in the western Pacific Ocean, is one of the most affected marginal seas by anthropogenic activities in the past 30 years, because its coastal cities witnessed the most rapid development of Chinese economy. The current system of the ECS mainly consists of a northward Kuroshio branch along the shelf-slope edge, the Taiwan Warm Current from the Taiwan Strait and the southward Zhejiang-Fujian Coastal Current along the coastline of Chinese mainland [1]. The Yangtze River is the primary sediment contributor of the ECS Shelf. Before 1980s, the ECS Shelf received about 4.8×10^8 tons of particulate matter from the Yangtze River every year [2]. Thereafter, the sediment load from the Yangtze River has significantly dropped because of a large number of dams were built which depressed the sediment transport [3, 4]. Due to the strong currents and tides in the ECS, the sedimentation of suspended particles on the shelf shows a fairly heterogeneous distribution pattern [5]. For example, there are two mud type sediment patches in the inner ECS Shelf and to the south of the Cheju Island [6–9]. Their sedimentation mechanisms and special impacts upon local ecosystems have been investigated by many researchers [3, 4, 8, 9]. Xu et al. [3] and Liu et al. [8, 9] examined the composition and source of inner shelf sediments. Huh et al. [5] and Su et al. [10] studied the sedimentary dynamics and budget of the ECS Shelf sediment using radionuclide tracers (^{137}Cs and ^{210}Pb). However, the lateral transports of dissolved and particulate matters are poorly understood, which prevent us from learning about the interactions between various areas and successive ecological effects over the ECS Shelf, especially after the building of the Three Gorges Dam which resulted in an apparent decreasing of sediment load and a wave of unexpected ecological variations on the ECS Shelf [11].

Published online: 22 May 2013

^{210}Pb is a strong particle reactive radionuclide with the half-life of 22.3 year. It has been proven to be an effective proxy of sedimentary process over centurial timescale in coastal and shelf regions [5, 10, 12]. Owing to its combination with particulate matters, ^{210}Pb is usually removed from the water column and settles into sediment. After being buried, ^{210}Pb decreases exponentially with time following its half-life, hence the activities of ^{210}Pb in deep sediment is lower than the surface sediment under steady state conditions. Because the decay of ^{210}Pb is independent of surrounding environments, the vertical profiles of ^{210}Pb in sediments record the sedimentation rates which can be used to quantify sedimentation of particulate matters in overlying water and subsequent lateral transport [10, 13].

To reveal the sedimentation and lateral transport of ^{210}Pb over the ECS Shelf, ^{210}Pb was determined in 11 surface sediment samples, as well as ^{210}Pb and ^{234}Th in the water columns at 4 stations. The focusing factor and mass balance models of ^{210}Pb were also used to quantitatively examine the boundary scavenging and resuspension processes.

Methods

Sampling sites

Three regions were selected for their specific sedimentation characteristics and geographical locations (Fig. 1). The coast, influenced by the Yangtze River plume, is generally regarded as a high sedimentation rate. However, whether it receives/provides sediments from/for the outer shelf has not been well understood. The mud region to the south of the Cheju Island has shown little variable sedimentation in the past 150 years [13], its sediment origins have been arguable to date. The southern shelf of the ECS, i.e. to the north of the Taiwan Strait, is the interface connecting the South China Sea (SCS) and the ECS. Seawater from the SCS and western Pacific Ocean, characterized by higher dissolved ^{210}Pb than the Taiwan Strait [14–16], has been directly transported into this region. Theoretically, boundary scavenging most probably occurs in this area. Thus, the three regions represent typical sediment environments on the ECS Shelf. Particle reactive ^{210}Pb might reveal insights into their sedimentation dynamics.

Analysis of ^{210}Pb and ^{226}Ra in sediment

Samples were collected from the top 0–3 cm surface sediment using a box-corer over the ECS Shelf (Table 1) and frozen at −20 °C. In the land laboratory, sediment samples were freeze dried and homogenized. Activities of ^{210}Pb and ^{226}Ra were measured by non-destructive gamma counting using a Canberra ultra-high purity germanium detector interfaced with a multi-channel analyzer, at 46.4 and 351.6 keV for ^{210}Pb and ^{226}Ra [17, 18], respectively. The net counts of ^{210}Pb and ^{226}Ra were more than 400 and 1,000 respectively, resulting in the statistical counting errors were <5 % for ^{210}Pb and 3 % for ^{226}Ra. The detector efficiencies were calibrated by standard materials [19]. All activities of ^{210}Pb and ^{226}Ra were corrected to the sampling time.

Analysis of ^{234}Th in the seawater

Four stations (i.e. S1002, S1004, S1008 and S0508) were selected to determine both ^{234}Th and ^{210}Pb in seawater. For ^{234}Th, 10 L of seawater at various depths were sampled by Niskin bottles. Particulate and dissolved ^{234}Th were immediately separated through GF/F filter. Two liters of filtrate were used to determine dissolved ^{234}Th [20, 21]. After adding NH_4OH to adjust the pH value to 9, right amounts of $KMnO_4$ and $MnCl_2{\cdot}4H_2O$ were successively added while stirring. The MnO_2 precipitate was settled for 6 h, and collected by GF/F filter. The filters, carrying particulate ^{234}Th and MnO_2, were dried at 60 °C. The activities of dissolved and particulate samples were measured by low background α/β counter. The errors were propagated from ±1 σ counting errors.

Analysis of ^{210}Pb in seawater

^{210}Pb in seawater was measured by α-spectrometry (ORTEC^{plus}) via its granddaughter of ^{210}Po. Detailed procedures were described by Yang et al. [22] and modified

Table 1 Sampling dates and the salinity of surface water at various stations

Station	Latitude (N)	Longitude (E)	Depth (m)	Surface salinity (psu)	Sampling date
F0502	31°25.254′	122°42.535′	43	33.591	2007-11-20
F0701	29°19.799′	122°14.745′	14	26.171	2007-11-19
F0703	29°07.664′	122°38.531′	54	34.063	2007-11-19
F0802	27°45.161′	121°26.885′	29	28.727	2007-11-16
F0803	27°38.453′	121°39.428′	46	33.504	2007-11-16
F1004	26°22.562′	121°18.246′	81	34.077	2007-11-15
FFJ-102	31°14.932′	125°51.470′	66	34.014	2007-11-08
FFJ-103	31°39.978′	125°51.671′	69	33.961	2007-11-07
FFJ-104	32°01.778′	125°52.358′	78	33.682	2007-11-07
C1002	26°43.253′	120°46.972′	48	33.931	2009-05-07
FJA	30°58.614′	122°40.651′	22	n.d.	2009-05-10
S1002	26°43.375′	120°47.103′	50	32.216	2006-06-28
S1004	26°22.563′	121°18.253′	79	33.074	2006-06-28
S1008	25°35.387′	122°36.512′	372	33.562	2006-06-30
S0508	30°50.765′	125°51.242′	75	32.453	2006-07-12

n.d. no data

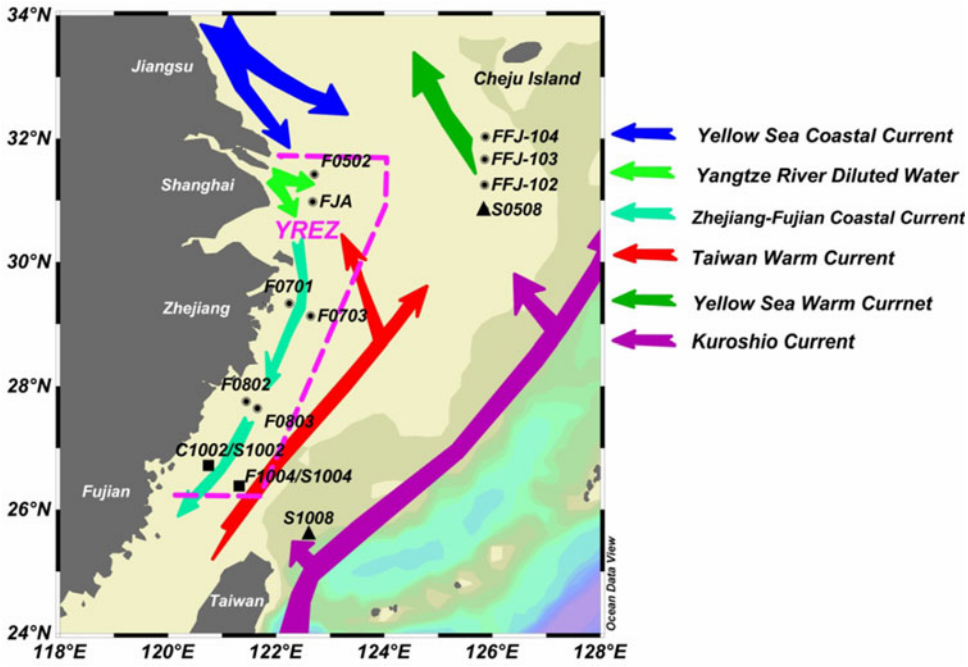

Fig. 1 Sampling stations on the ECS Shelf, *circles* denote only surface sediments were collected, *triangles* denote only water samples were collected and *square* means both sediments and water were collected; *arrows* represent the primary circulation in the ECS, YREZ namely Yangtze River Estuary Zone

in this study. Briefly, 5 L of seawater was filtered through polycarbonate membrane filter with 0.4 μm pore size. The filtrate, i.e. dissolved ^{210}Pb, was acidified with 4 mol L^{-1} nitric acid to pH < 1, and then Fe^{3+} carrier ($FeCl_3$), quantified Pb^{2+} and ^{209}Po were added as ^{210}Pb and ^{210}Po yield tracers. After 24 h, ammonia was added to adjust the pH value to 9, Po and Pb were co-precipitated with $Fe(OH)_3$, which was collected by settling and centrifugation. The precipitation was dissolved with HCl. By adjusting the pH value to 1.5 and adding ascorbic acid to combine Fe^{3+}, Po isotopes (^{209}Po and ^{210}Po) were plated onto a sliver disc at 90 °C for 4 h. Particulate samples were digested by mixed acid (i.e.HNO_3, $HClO_4$ and HF) after Pb and Po spikes were added. The following plating procedures of polonium isotopes were the same as used for the dissolved samples. ^{210}Pb in both dissolved and particulate samples were determined by ingrowth ^{210}Po after 1.5 years. The chemical yield of ^{210}Pb was determined by stable lead measured by atomic absorption spectrometry. The net counts of ^{210}Po were more than 400, thus the counting errors were <±5 %.

Results and discussion

Excess ^{210}Pb

Excess ^{210}Pb (i.e. $^{210}Pb_{ex}$), exceeding its grandparent of ^{226}Ra, is the unsupported ^{210}Pb, which can be quantified by subtracting ^{226}Ra activity from the total ^{210}Pb. Generally, $^{210}Pb_{ex}$ in sediment is from ^{210}Pb combined with particulate matter in overlying seawater due to its stronger particle reactivity contrasting with ^{226}Ra. Because $^{210}Pb_{ex}$ decayed after sedimentation, comparison of $^{210}Pb_{ex}$ activities at different sites requires normalization back to its initial deposition time. In our study, the top 3 cm sediment was collected, thus the measured activities of $^{210}Pb_{ex}$ need to be corrected according to the sedimentation rates at corresponding stations.

Provided that A_i is the $^{210}Pb_{ex}$ activity for infinitesimal layer (i), it can be expressed as

$$A_i = A_0 e^{-\lambda t_i} \quad (1)$$

where A_0 represents the $^{210}Pb_{ex}$ activity when ^{210}Pb sinks into sediment (i.e. $^{210}Pb^0_{ex}$ in dpm g^{-1}), t_i denotes the age of i layer (year). In a steady state, the inventory of $^{210}Pb_{ex}$ (i.e. I in dpm cm^{-2}) in the top 3 cm sediment can be calculated by

$$I = \int_0^T A_i m_v dt = \int_0^T A_0 m_v e^{-\lambda t} dt \quad (2)$$

where m_v represents the sediment accumulation rate in g cm^{-2} $year^{-1}$, which were constrained by ^{137}Cs [10, 23], T is the deposit time for the top 3 cm sediment. Based on our measurements, the inventory of excess ^{210}Pb can be expressed as

$$I = A_m M \quad (3)$$

where A_m represents the measured excess ^{210}Pb activity in the top 3 cm sediments (dpm g^{-1}) and M denotes the dry weight of sediment in g cm^{-2} (Table 2). Combining the Eqs. (2) and (3),

Table 2 Activities of ^{210}Pb and ^{226}Ra in sediments and fluxes of ^{210}Pb calculated from mass balance model in the water column

Station	^{210}Pb (dpm g^{-1})	^{226}Ra	$^{210}Pb_{ex}^{ma}$	$^{210}Pb_{ex}^{0a}$	M (g cm^{-2})	m_v^b (g cm^{-2} year^{-1})	F_{sed} (dpm cm^{-2} year^{-1})	F_{Ra}	$F_{boundary}$	f
F0502	1.50 ± 0.14	0.95 ± 0.09	0.5 ± 0.2	0.6 ± 0.2	3.8	0.4	0.23 ± 0.08	0.017 ± 0.001	−1.58 ± 0.08	0.20
F0701	1.77 ± 0.17	1.09 ± 0.10	0.7 ± 0.2	0.7 ± 0.2	3.6	0.9	0.67 ± 0.18	0.007 ± 0.001	−1.13 ± 0.18	0.58
F0703	3.97 ± 0.34	1.04 ± 0.10	2.9 ± 0.4	3.0 ± 0.4	3.6	0.98	3.01 ± 0.39	0.019 ± 0.002	1.20 ± 0.39	2.58
F0802	1.78 ± 0.17	1.00 ± 0.09	0.8 ± 0.2	1.0 ± 0.2	3.6	0.31	0.30 ± 0.06	0.014 ± 0.001	−1.51 ± 0.06	0.26
F0803	5.44 ± 0.47	1.21 ± 0.11	4.2 ± 0.5	6.3 ± 0.8	3.4	0.12	0.76 ± 0.10	0.022 ± 0.001	−1.05 ± 0.10	0.65
F1004	5.66 ± 0.47	1.36 ± 0.12	4.3 ± 0.5	5.0 ± 0.6	3.9	0.39	1.95 ± 0.23	0.020 ± 0.003	0.14 ± 0.23	1.67
FFJ-102	2.18 ± 0.20	1.69 ± 0.14	0.5 ± 0.2	0.6 ± 0.2	3.6	0.25	0.16 ± 0.05	0.026 ± 0.001	−1.66 ± 0.05	0.14
FFJ-103	1.16 ± 0.11	0.74 ± 0.07	0.4 ± 0.1	0.5 ± 0.1	3.4	0.2	0.10 ± 0.02	0.027 ± 0.001	−1.72 ± 0.02	0.08
FFJ-104	1.69 ± 0.17	0.85 ± 0.08	0.8 ± 0.2	1.0 ± 0.2	3.4	0.3	0.29 ± 0.06	0.030 ± 0.002	−1.54 ± 0.06	0.25
C1002	7.17 ± 0.67	2.00 ± 0.19	5.2 ± 0.7	6.0 ± 0.8	3.6	0.4	2.39 ± 0.32	0.022 ± 0.001	0.57 ± 0.32	2.04
FJA	4.23 ± 0.42	1.08 ± 0.11	3.2 ± 0.4	3.7 ± 0.5	3.6	0.4	1.47 ± 0.20	0.010 ± 0.001	−0.33 ± 0.20	1.27

[a] $^{210}Pb_{ex}^{m}$ and $^{210}Pb_{ex}^{0}$ denote the measured and time normalized values of excess ^{210}Pb, respectively

[b] Sediment rates were from Su and Huh [10]

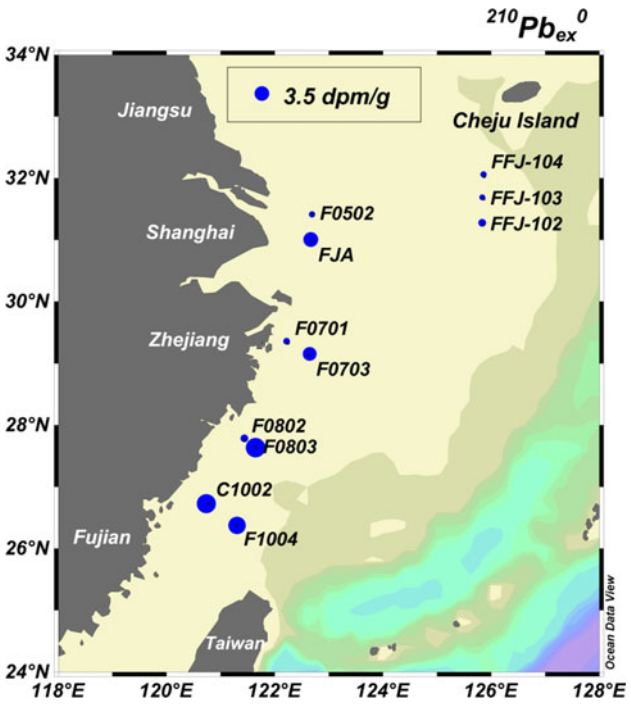

Fig. 2 Distribution pattern of $^{210}Pb_{ex}^{0}$ over the East China Sea Shelf

$$A_m M = \int_0^T A_0 e^{-\lambda t} m_v dt \tag{4}$$

Because the sedimentation time of the top 3 cm sediment (i.e. T) can be constrained by M and m_v (i.e.$T = M/m_v$), A_0 can be acquired by the following equation

$$A_0 = A_m \frac{\lambda M}{m_v(1 - e^{-\lambda M/m_v})} \tag{5}$$

The specific activities of excess ^{210}Pb over the ECS Shelf varied from 0.5 to 6.3 dpm g^{-1} with an average of 2.6 dpm g^{-1} (Table 2), which was close to the values in the East Malaysia coastal sediments [24]. The result at C1002 station was also comparable with that obtained in its adjacent region [25]. Overall, $^{210}Pb_{ex}^{0}$ was low at inshore stations, and it increased towards outer shelf (Fig. 2). The large variability of $^{210}Pb_{ex}^{0}$, spanning an order of magnitude, indicated that ^{210}Pb sedimentation over the ECS shelf has a fairly heterogeneous spatial distribution pattern. Because excess ^{210}Pb in the ECS sediments predominantly resulted from the atmospheric deposition of ^{210}Pb [5, 10], which showed little spatial variability [10, 26], the heterogeneity of $^{210}Pb_{ex}^{0}$ potentially revealed the significant spatial variations in ^{210}Pb sedimentation and thus combined particulate matters.

Focusing factor of ^{210}Pb (f)

The focusing factor (f), defined as the ratio of interested nuclide inventory within an interval of sediment to the

production of the interested nuclide in the overlying water column over the time of accumulation [27, 28], was used to quantify the efficiency of ^{210}Pb sedimentation from the water column to local sediment [29, 30]. The f values of $^{210}Pb_{ex}$ can be described by

$$f = \frac{F_{sed}}{F_{atm} + F_{Ra} - F_{decay}} \quad (6)$$

where F_{atm} and F_{sed} denote the atmospheric flux and sedimentation flux of ^{210}Pb (dpm cm^{-2} year^{-1}), respectively. F_{Ra} is the production flux of ^{210}Pb from ^{226}Ra in the water column (dpm cm^{-2} year^{-1}); F_{decay} is the disintegration term of ^{210}Pb in the water column (dpm cm^{-2} year^{-1}). Hence, the input and production of ^{210}Pb in the overlying water column will completely sink to local sediment when the f is equal to unity. In other words, there is no lateral transport of ^{210}Pb or the net effect of lateral transport is neglectable. If the f value is greater than 1.0, part of ^{210}Pb, from other sites through lateral transport, would settle down the studied site. The <1.0 f values imply that part of ^{210}Pb at the studied site, as a source, is transported to other sites.

The atmospheric deposition of ^{210}Pb over the ECS has been little investigated. Thus, the depositional fluxes of ^{210}Pb at near shore stations around the ECS were adopted. From the northern city (Qingdao) to the southern site (Xiamen), the atmospheric fluxes of ^{210}Pb varied from 0.7 to 1.15 dpm cm^{-2} year^{-1} in the past 15 years [10, 26, 31, 32]. To conservatively estimate the lateral transport of ^{210}Pb over the ECS Shelf, 1.15 dpm cm^{-2} year^{-1} was adopted as the upper limit of the ^{210}Pb depositional flux in this study. On the basis of the inventory of ^{210}Pb in the water column at four stations and the upper limit residence time of ^{210}Pb, F_{decay} was estimated to be <3 % of the F_{atm} term and thus it was neglected. The values of F_{Ra} can be calculated by the ^{226}Ra activities of the same cruise [33]. The term of F_{sed} can be acquired by Eq. (7)

$$F_{sed} = A_0 m_v = A_m \frac{\lambda M m_v}{m_v(1 - e^{-\lambda M/m_v})} \quad (7)$$

The F_{sed} values varied from 0.10 to 3.01 dpm cm^{-2} year^{-1} with the mean of 1.03 dpm cm^{-2} year^{-1} (Table 2). In comparison, it ranged from 0.29 to 1.26 dpm cm^{-2} year^{-1}, averaging 0.68 dpm cm^{-2} year^{-1} [5] if ^{210}Pb preserved for five halves (111.5 years) in sediments. Our higher results were ascribed to the more coastal stations which received much more riverine ^{210}Pb than the inner and mid-shelf regions mainly covered by [5]. The values of f ranged between 0.08 and 2.58 with an average of 0.88 (Table 2, Fig. 3). In general, the f values increased southwards along the inner shelf, indicating that sedimentation efficiencies of ^{210}Pb were comparatively higher in the southern area.

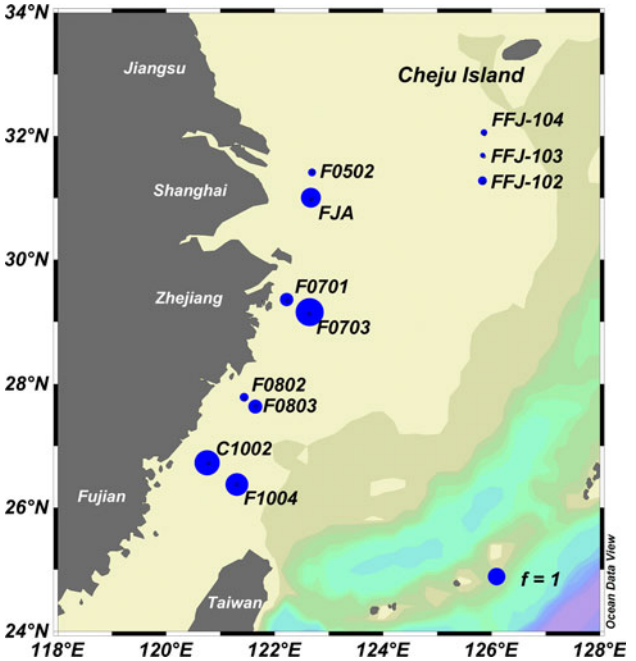

Fig. 3 Focusing factors of ^{210}Pb on the ECS Shelf, the size of *circles* represent the value of focusing factor

However, the f value at F0703 station (2.56) was exceptionally higher than the southern stations such as C1002 and F1004 with the f values of 2.04 and 1.67, respectively. Therefore, lateral transport contribution of ^{210}Pb to the F0703 station was much more evident. In contrast, the f values were much less than unity at stations of FFJ-102, FFJ-103 and FFJ-104 (0.14, 0.08 and 0.25 for three stations, respectively), revealing that only part of the atmospheric deposition of ^{210}Pb settled into local sediment, the majority of ^{210}Pb was transported to other area probably resulted from sediment resuspension and strong current (i.e. Yellow Sea Warm Current).

Lateral transport of ^{210}Pb over the ECS shelf

Evident lateral transport of ^{210}Pb has been observed in the ECS as approved by the focusing factors. Theoretically, two potential sources might contribute ^{210}Pb through lateral transport. One is the Yangtze River plume, which carries amount of terrestrial material including ^{210}Pb. The other is the boundary scavenging induced by the horizontal advection and diffusion of higher ^{210}Pb water masses from the western Pacific Ocean and the South China Sea. Thus, a mass balance model was adopted to quantify this lateral transport of ^{210}Pb including river contribution and boundary scavenging terms [10],

$$\frac{\partial I_{Pb}}{\partial t} = F_{atm} + F_{river} + F_{Ra} + F_{boundary} - F_{sed} - F_{decay} \quad (8)$$

where I_{Pb} is the inventory of ^{210}Pb in the water column, F_{river} and $F_{boundary}$ represent the input flux of ^{210}Pb from the Yangtze River and the boundary scavenging flux of ^{210}Pb (dpm cm^{-2} year^{-1}). With the steady state assumption,

$$F_{boundary} = F_{sed} + F_{decay} - F_{atm} - F_{river} - \lambda_{Pb} I_{Ra} \quad (9)$$

where λ_{Pb} is the decay constant of ^{210}Pb (0.031 year^{-1}) and I_{Ra} represents the inventory of ^{226}Ra in the water column (dpm m^{-2}). ^{210}Pb derived from the Yangtze River was 0.64 dpm cm^{-2} year^{-1} [12]. The boundary scavenging flux of ^{210}Pb, then, was evaluated by Eq. (9).

The $F_{boundary}$ values at F0502 and FJA stations were −1.58 and −0.33 dpm cm^{-2} year^{-1} respectively (Table 2), indicating net lateral export of ^{210}Pb from the two stations to other sites. Notably, although locating near the mouth of the Yangtze River the $F_{boundary}$ value of F0502 was fourfold lower than FJA. The difference was ascribed to the topography and different sediment types between F0502 and FJA. On one hand, there is a submarine canyon between the mouth of the Yangtze River and F0502 [10]. The northwest branch of the Taiwan Warm Current (TWC) induces an upwelling system all the year round when it reaches the canyon [34–36], which is stronger than the Yangtze River plume and impedes the Yangtze river derived sediments to cross over the submarine canyon [10, 36]. On the other hand, FJA is located at the rim of Qiantang mud patch where sediment is mainly composited of silt/clay (Fig. 4), which is characterized by small size, large surface area and thus more adsorbed ^{210}Pb [37, 38].

For the costal stations close to Zhejiang Province, the highest $F_{boundary}$ of 1.20 dpm cm^{-2} year^{-1} was observed at F0703 station (Table 2), followed by F0701 and F0803 with values of −1.13 and −1.05 dpm cm^{-2} year^{-1}, respectively. F0802 represents the minimum boundary scavenging of ^{210}Pb. The $F_{boundary}$ of ^{210}Pb at F0703 (> 0) indicated that this station acquired a large amount of boundary scavenged ^{210}Pb from open water. On the contrary, other three stations, as source sites, exported amounts of ^{210}Pb to the outer shelf. This contrasting scenario was attributed to the upwelling at F0703. Men et al. [39], based on ^{224}Ra isotope, stated that the vertical eddy diffusion coefficients at F0703 (163 and 84.6 cm^2 s^{-1} in winter and summer respectively) were several-fold higher than the average of this area (35.9 cm^2 s^{-1}), supporting the upwelling at F0703. The upwelling carries abundant nutrients to the surface water and consequently more biogenic particulate matter. Due to the strong particle reactivity of ^{210}Pb, the upwelling would result in efficient sedimentation of ^{210}Pb at F0703. At the same time, the upwelling also caused the convergence of fine-grained sediments as revealed by the mud type of sediment [40, 41], which also favor to enrich ^{210}Pb.

The values of $F_{boundary}$ were 0.57 and 0.14 dpm cm^{-2} year^{-1} at C1002 and F1004 respectively, which accounted for 31 and 8 % of the total ^{210}Pb input to the overlying water column at the two stations. These values were actually underestimated because the two stations are in the far south of the Yangtze River Estuary, the river contribution should be less than the input of 0.64 dpm cm^{-2} year^{-1} from

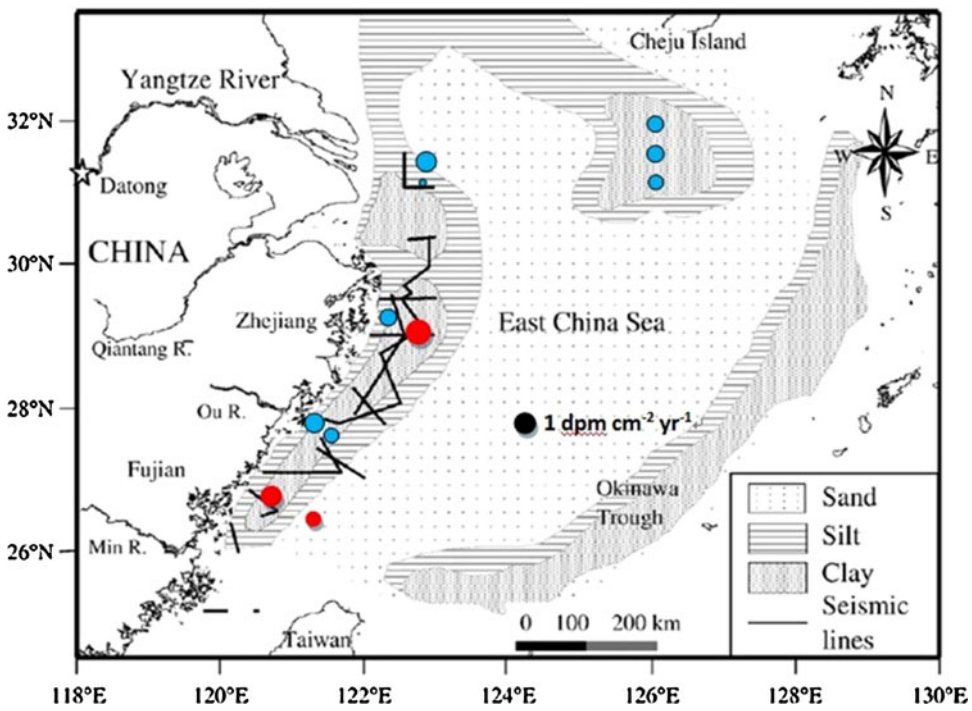

Fig. 4 The boundary scavenge flux of ^{210}Pb ($F_{boundary}$) on the ECS Shelf (sediment types refer to [9]). *Red* and *blue* circles represent positive and negative values respectively, while the size of *circle* represents the value of $F_{boundary}$

the river mouth as was adopted in this study. Geographically, the boundary scavenged ^{210}Pb at C1002 and F1004 most likely came either from the South China Sea water through the Taiwan Strait, or from the western Pacific Ocean water via a branch of Kuroshio into the ECS. Overall, the southern area of the ECS was a sink of ^{210}Pb, acquiring a considerable amount of boundary scavenged ^{210}Pb.

To quantitatively examine whether the region, influenced by the Yangtze River plume (called the Yangtze River Estuary Zone, i.e. YREZ), is an overall source/sink of ^{210}Pb, eight coastal stations, situated in the plume zone, were selected (Fig. 1) based on the distribution of ^{228}Ra [41].The $F_{boundary}$ values of eight stations varied from -1.58 to 1.20 dpm cm^{-2} year^{-1} with an average of -0.46 dpm cm^{-2} year^{-1} (Table 2). By introducing the discharge of the Yangtze River [12], the budget of ^{210}Pb in the YREZ suggested that about 25 % of the total ^{210}Pb was exported to the outer shelf (Fig. 5), revealing the YREZ as a source area of ^{210}Pb. Du et al. [12] reported that 35 % of the total ^{210}Pb was transported to outer shelf, which was slightly higher than our result. This difference was ascribed to the defined different zone. In our study, the YREZ extended to 26°N whereas the southern borderline was 27°N in the research conducted by Du et al. [12]. The southmost stations (i.e. C1002 and F1004) actually acquired boundary scavenged ^{210}Pb; in consequence, they resulted in a low value in our study compared with Du et al. [12]. Because ^{210}Pb is a strong particle reactive nuclide, the lateral export of ^{210}Pb from the YREZ revealed that amounts of suspended particulate matter transported from the coastal area to outer shelf. In fact, several investigations provided evidence for this scenario. For example, McKee et al. [42] proposed that terrestrial sediment deposited near the Yangtze River mouth in summer could be eroded and transported southwards in winter with frequent storms. Fan et al. [43] found that the Yangtze River derived sediment on the ECS Shelf decreased towards outer shelf which confirmed the transport of particle materials from the Yangtze River mouth.

In addition, the sedimentation of ^{210}Pb has a close relation with the sediment type. Stations in the mud zone (i.e. FJA, F0703, F0803 and C1002) showed a higher average $^{210}Pb^{0}_{xs}$ activity of 4.76 dpm g^{-1}, while low $^{210}Pb^{0}_{xs}$ values were observed at stations situated in non-mud zone (Fig. 4). Thus, the mud sediment zone in the coastal region [8, 9, 44] was probably the main ^{210}Pb sedimentation area in the YREZ.

The $F_{boundary}$ values were -1.66, -1.72 and -1.54 dpm cm^{-2} year^{-1} for FFJ-102, FFJ-103 and FFJ-104, respectively (Table 2), indicating that <20 % of input ^{210}Pb settled into local sediment. The majority of ^{210}Pb was exported to other area through lateral transport, which may be caused by the resuspension of sediment. Previous researches suggested that the sediments at these stations were easily re-suspended by the Yellow Sea Warm Current [45] and finally reached the coast of the Korea peninsula [46].

Lateral transport of ^{210}Pb constrained by ^{234}Th and ^{210}Pb in seawater

Because $^{210}Pb_{ex}$ in sediment was from the overlying seawater, the vertical export of ^{210}Pb from the water column, theoretically, can also reveal the lateral transport of ^{210}Pb, along with its source terms. At four stations (Fig. 6), ^{234}Th, ^{210}Pb and ^{238}U (via salinity [47]) were determined to quantify the export of ^{210}Pb from the water column. Overall, ^{234}Th was deficit to its grandparent of ^{238}U, hence the disequilibria between ^{234}Th and ^{238}U can be used to trace the export of ^{210}Pb. The export fluxes of ^{234}Th were evaluated by the model

$$\frac{\partial I_{Th}}{\partial t} = \lambda_{Th} I_U - \lambda_{Th} I_{Th} - F_{Th} \quad (10)$$

where I_{Th} and I_U were the inventories of ^{234}Th and ^{238}U in the water column, respectively. F_{Th} is the vertical export flux of ^{234}Th. The residence time of ^{234}Th then can be calculated by I_{Th} and F_{Th} under a steady state (I_{Th}/F_{Th}). ^{234}Th and ^{210}Pb were assumed to have the same residence

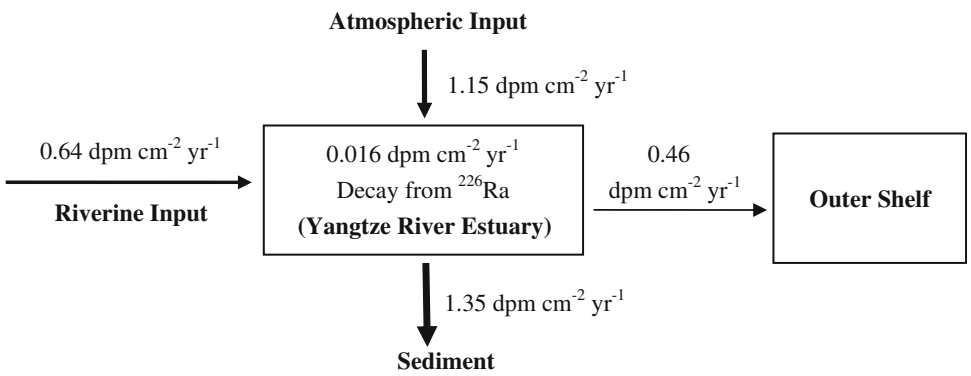

Fig. 5 The budget of ^{210}Pb constrained by mass balance model in the Yangtze River plume zone

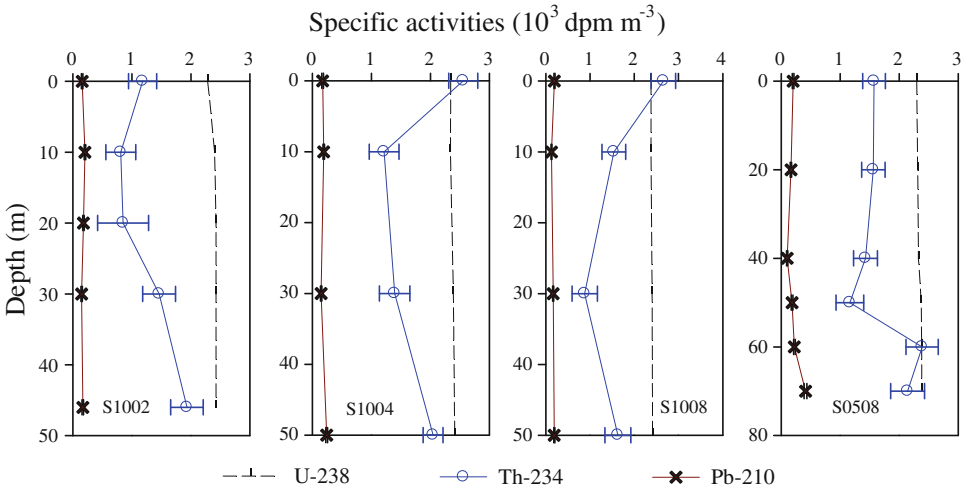

Fig. 6 Specific activities of ^{210}Pb and ^{234}Th in the water column over the East China Sea Shelf

Table 3 Vertical export fluxes and lateral transport of ^{210}Pb quantified by ^{234}Th-^{210}Pb approach

Station	Export interface (m)	I_{Th} (10^4 dpm m^{-2})	I_{Pb} (10^3 dpm m^{-2})	F_{Th} (10^3 dpm m^{-2} d^{-1})	F_{Pb} (dpm cm^{-2} $year^{-1}$)	F_{adv}
S1002	46	5.39 ± 0.49	7.62 ± 0.19	1.46 ± 0.14	7.54 ± 1.07	6.39 ± 1.07
S1004	50	7.93 ± 0.51	9.04 ± 0.28	1.08 ± 0.14	4.49 ± 0.69	3.34 ± 0.69
S1008	50	7.03 ± 0.60	8.20 ± 0.24	1.39 ± 0.17	5.91 ± 0.91	4.76 ± 0.91
S0508	70	8.68 ± 0.80	10.08 ± 0.54	2.12 ± 0.23	8.98 ± 1.20	7.83 ± 1.20

time due to their similar particle reactivity. Therefore, the lateral transport of ^{210}Pb (F_{adv}) can be estimated by the inventory of ^{210}Pb in seawater and its residence time,

$$F_{adv} = F_{Pb} - F_{atm} = \frac{I_{Pb}}{I_{Th}/F_{Th}} - F_{atm} \quad (11)$$

where F_{Pb} represent the vertical export flux of ^{210}Pb in dpm cm^{-2} $year^{-1}$ (Table 3).

The lateral transport of ^{210}Pb, including river input and boundary scavenging, varied from 3.34 to 6.39 dpm cm^{-2} $year^{-1}$ for stations to the north of the Taiwan Strait (i.e. S1002, S1004 and S1008). By subtracting the overestimated river contribution of 0.64 dpm cm^{-2} $year^{-1}$, the boundary scavenging of ^{210}Pb ranged between 2.70 and 5.75 dpm cm^{-2} $year^{-1}$ with an average of 4.19 dpm cm^{-2} $year^{-1}$. The Taiwan Warm Current may be the main carrier of boundary scavenged ^{210}Pb. There is a net water transport of 1.0-2.1 Sv (1 Sv = 10^6 m^3 s^{-1}) through the Taiwan Strait to the ECS [48–50]. In addition, the specific activity of ^{210}Pb in the surface water increased offshore (Fig. 6), ^{210}Pb activity in the northwestern Pacific Ocean were 3–5 times higher than the values in the ECS [51]. These comparisons also supported ^{210}Pb may diffuse into the ECS directly from the western Pacific Ocean.

The vertical export fluxes of ^{210}Pb (i.e. F_{Pb}), derived from the ^{234}Th-^{210}Pb approach, varied from 4.49 to 7.54 dpm cm^{-2} $year^{-1}$ with the mean of 5.98 dpm cm^{-2} $year^{-1}$ for the stations to the north of the Taiwan Strait (Table 3). Comparing with ^{210}Pb mass-balance method in sediment, F_{Pb} was higher than the averaged F_{sed} of 2.17 dpm cm^{-2} $year^{-1}$. The exported ^{210}Pb must experience remineralization and resuspension before buried in sediment [52], consequently resulting in lower sedimentation fluxes contrasting with the export fluxes from the overlying water column. Thus, the difference between F_{Pb} and F_{sed} can be used to quantify the remineralization of settling particles or/and resuspension of sediment. About 47–74 % of vertically exported ^{210}Pb from the water column did not settle to local sediment at stations to the north of the Taiwan Strait. In spite of the difference between the two methods, they both indicated evident boundary scavenging to the north of the Taiwan Strait.

The F_{Pb} value was 8.98 dpm cm^{-2} $year^{-1}$ for S0508 station. Assuming S0508 had the same F_{sed} as its adjacent stations (FFJ-102, FFJ-103 and FFJ-104), only <4 % of the vertical exported ^{210}Pb from the overlying water was finally buried in local sediment. The majority of the vertical exported ^{210}Pb was transported to other sites, coinciding with our conclusion drawn from sediment that strong hydrodynamic conditions led amounts of settled ^{210}Pb to be re-suspended and subsequently relocated.

Conclusions

(1) Excess ^{210}Pb in sediments showed significantly heterogeneous spatial pattern over the East China Sea

Shelf. Overall, the north to the Taiwan Strait is a sink area of ^{210}Pb, whereas the coastal area covered by the Yangtze River plume and the south to the Cheju Island are source regions of ^{210}Pb.

(2) To identify the provenance of lead isotopes in the East China Sea, boundary scavenging of Pb must be considered due to its significant contribution.

(3) It may be efficient way to quantify the remineralization and resuspension effect over the shelf using the flux difference of ^{210}Pb between its vertical export from the overlying water column and sedimentation.

Acknowledgments We appreciate Professor Tibor Braun and tow anonymous reviewers for their constructive suggestions, which greatly improved the presentation of this manuscript. This work is supported jointly by a Chinese COMRA program (No. DY125-13-E-01) and the Chinese National Science Foundation (41076043 and 41125020).

References

1. Gao S, Jia JJ (2003) Modeling suspended sediment distribution in continental shelf upwelling/down welling settings. Geo Mar Lett 22:218–226
2. Milliman JD, Meade RH (1983) World-wide delivery of sediment to the oceans. J Geology 91(3):1–21
3. Xu KH, Milliman JD (2009) Seasonal variations of sediment discharge from the Yangtze River before and after impoundment of the Three Gorges Dam. Geomorph 104:276–283
4. Xu KH, Milliman JD, Li AC, Liu JP, Kao SJ, Wan SM (2009) Yangtze- and Taiwan-derived sediments on the inner shelf of East China Sea. Cont Shelf Res 29:2240–2256
5. Huh CA, Su CC (1999) Sedimentation dynamics in the East China Sea elucidated from ^{210}Pb, ^{137}Cs and ^{239,240}Pu. Mar Geol 160:183–196
6. Guo ZG, Yang ZS, Lei K, Qu YH, Fan DJ (1999) Seasonal variation of the sedimentary dynamic processes for the mud area in the northern East China Sea. J Ocean Univ Qingdao 29(3): 507–513 (in Chinese)
7. Lei K, Yang ZS, Guo ZG (2001) Sedimentation with aggregation of suspended sediment in a mud area of the northern East China Sea. Oceanol Limnol Sin 32(3):288–295 (in Chinese)
8. Liu JP, Li AC, Xu KH, Velozzi DM, Yang ZS, Milliman JD, DeMaster DJ (2006) Sedimentary features of the Yangtze River-derived along-shelf clinoform deposit in the East China Sea. Cont Shelf Res 26:2141–2156
9. Liu JP, Xu KH, Li AC, Milliman JD, Velozzi DM, Xiao SB, Yang ZS (2007) Flux and fate of Yangtze River sediment delivered to the East China Sea. Geomorph 85:208–224
10. Su CC, Huh CA (2002) ^{210}Pb, ^{137}Cs and ^{239,240}Pu in East China Sea sediments: sources, pathways and budgets of sediments and radionuclides. Mar Geol 183:163–178
11. Jiao N, Zhang Y, Zeng Y, Gardner WD, Mishonov AV, Richardson MJ, Hong N, Pan D, Yan X-H, Jo Y-H, Chen C-TA, Wang P, Chen Y, Hong H, Bai Y, Chen X, Huang B, Deng H, Shi Y, Yang D (2007) Ecological anomalies in the East China Sea: impacts of the Three Gorges Dam? Water Res 41:1287–1293
12. Du JZ, Wu YF, Huang YF, Zhang J (2010) Use of ^{7}Be, ^{210}Pb and ^{137}Cs tracers to the transport of surface sediments of the Changjing Estuary, China. J Mar Sys 82:286–294
13. Yang W, Chen M, Li G, Cao J, Guo Z, Ma Q, Liu J, Yang J (2009) Relocation of the Yellow River as revealed by sedimentary isotopic and elemental signals in the East China Sea. Mar Pollut Bull 58:923–927
14. Yang W (2005) Marine biogeochemistry of ^{210}Po and ^{210}Pb and their implications regarding the cycling and export of particles. Ph.D. dissertation, Xiamen University, 176–211 (in Chinese)
15. Yang W, Huang Y, Chen M, Zhang L, Li H, Liu G, Qiu Y (2006) Disequilibria between ^{210}Po and ^{210}Pb in surface waters of the southern South China Sea and their implications. Sci China Ser D 49:103–114
16. Wei CL, Chou LH, Tsai JR, Wen LS, Pai SC (2009) Comparative Geochemistry of 234Th, 210Pb and 210Po: a case study in the Hung-Tsai Trough off Southwestern Taiwan. Terr Atmos Ocean Sci 20(2):411–423
17. Yao SC, Li SJ, Zhang HC (2008) ^{210}Pb and ^{137}Cs dating of sediments from Zigetang lake, Tibetan Plateau. J Radioanal Nucl Chem 278:55–58
18. Gelen A, Soto J, Gómez J, Díaz O (2004) Sediment dating of Santander Bay, Spain. J Radioanal Nucl Chem 261:437–441
19. Liu GS, Huang YP (1998) Simultaneous measurement of ^{238}U, ^{235}U, ^{210}Pb, ^{228}Th, ^{228}Ra, ^{226}Ra, ^{60}Co and ^{137}Cs in sediment samples using HP Ge γ spectrometer. J Oceanogr Taiwan Strait 17(4):359–363 (in Chinese)
20. Ma Q, Chen M, Qiu YS, Huang YP (2005) MnO_2 precipitation and direct beta counting technique for determining ^{234}Th in small volume seawater. Acta Oceanol Sin 27(4):68–75 (in Chinese)
21. Benitez-Nelson CR, Buesseler KO, Rutgers van der Loeff M, Andrews J, Ball L, Crossin G, Charette MA (2001) Testing a new small-volume technique for determining ^{234}Th in seawater. J Radioanal Nucl Chem 248:795–799
22. Yang W, Guo L, Chuang C-Y, Schumann D, Ayranov M, Santschi PH (2013) Adsorption characteristics of ^{210}Pb, ^{210}Po and ^{7}Be onto micro-particle surfaces and the effects of macromolecular organic compounds. Geochim Cosmchim Acta 107:47–64
23. Pan SM, Xu YH, Wang A, Povinec PP (2012) The ^{137}Cs distribution in sediment profiles from the Yangtze River estuary: a comparison of modeling and experimental results. J Radioanal Nucl Chem 292:1207–1214
24. Mahmood ZUW, Mohamed CAR, Ishak AK, Bakar NSA, Ishak K (2011) Vertical distribution of ^{210}Pb and ^{226}Ra and their activity ratio in marine sediment core of the East Malaysia coastal waters. J Radioanal Nucl Chem 289:953–959
25. Li DM, Xu MQ, Liu GS, Li C (2007) Distribution of radioisotopes in sediment cores from nearshore off Xinghua Bay mouth, Fujian, China. J Radioanal Nucl Chem 273:151–155
26. Yi Y, Zhou P, Liu GS (2007) Atmospheric deposition fluxes of ^{7}Be, ^{210}Pb and ^{210}Po at Xiamen, China. J Radioanal Nucl Chem 273:157–162
27. Singh AK, Marcantonio F, Lyle M (2011) Sediment focusing in the Panama Basin, Eastern Equatorial Pacific Ocean. Earth Planet Sci Lett 309:33–44
28. Suman DO, Bacon MP (1989) Variations in Holocene sedimentation in the North-American basin determined from Th-230 measurements. Deep-Sea Res I 36(6):869–878
29. Chen M, Ma Q, Guo LD, Qiu YS, Huang YP, Yang WF (2012) Importance of lateral transport processes to ^{210}Pb budget in the eastern Chukchi Sea during summer 2003. Deep-Sea Res II 81–84:53–62
30. Cochran JK, McKibbin-Vaughan T, Dornblaser MM, Hirschberg D, Livingston H, Buesseler KO (1990) ^{210}Pb scavenging in the North Atlantic and North Pacific Oceans. Earth Planet Sci Lett 97:332–352
31. Yi Y, Bai J, Liu G, Yang W, Yi Q, Huang Y, Chen H (2005) Measurements of atmospheric deposition fluxes of ^{7}Be, ^{210}Pb and ^{210}Po. Mar Sci 29:20–24 (in Chinese)

32. Su C-A, Huh C-A, Lin F-J (2003) Factors controlling atmospheric fluxes of ^{7}Be and ^{210}Pb in northern Taiwan. Geophys Res Lett 30(19):2018. doi:10.1029/2003GL018221
33. Men W (2008) The study on the oceanography of the Yellow Sea and the East China Sea traced by radium isotopes. Ph.D. dissertation, Xiamen University, 71–123 (in Chinese)
34. Jacobs GA, Hur HB, Riedlinger SK (2000) Yellow and East China Seas response to winds and currents. J Geophys Res 105:21947–21968
35. Zhao BR (1993) Upwelling off the Changjiang river mouth. Acta Oceanol Sin 15(2):108–114 (in Chinese)
36. Guo ZG, Yang ZS, Zhang DQ, Fan DJ, Lei K (2002) Seasonal distribution of suspended matter in the northern East China Sea and barrier effect of current circulation on its transport. Acta Oceanol Sin 24(5):71–80 (in Chinese)
37. Chung Y, Chang HC, Hung GW (2004) Particulate flux and ^{210}Pb determined on the sediment trap and core samples from the northern South China Sea. Cont Shelf Res 24:672–691
38. Ye YG, He J, Diao SB, Cai SQ, Song SQ (1992) Standardization of ^{210}Pb profile in the modern Huanghe river delta-the correlation method of grain size. Sci Geograph Sin 12(4):279–286 (in Chinese)
39. Men W, Wang FF, Liu GS (2011) ^{224}Ra and its implications in the East China Sea. J Radioanal Nucl Chem 288:189–197
40. Qu TD, Hu DX (1993) Upwelling and sedimentary dynamics II. A simple model. Chinese J Oceanol Limol 11(2): 289–295
41. Men W, Liu GS, Huang YP (2010) Measurement of ^{228}Ra in the Yellow Sea and East China Sea using the radon emanation method. J Radioanal Nucl Chem 284:65–72
42. Mckee BA, Nittrouer CA, DeMaster DJ (1983) Concepts of sediment deposition and accumulation applied to the continental shelf near the mouth of the Yangtze River. Geology 11:631–633
43. Fan DJ, Yang ZS, Sun XG, Zhang DQ, Guo ZG (2002) Quantitative evaluation of sediment provenance on the north area of the East China Sea shelf. J Ocean Univ Qingdao 32(5):748–756 (in Chinese)
44. Qin YS (1979) A study on sediment and mineral compositions of the floor of the East China Sea. Ocean Sel 2(2):130–142
45. Lei K, Yang ZS, Guo ZG, Bai H (2001) Suspended sediment flux in spring on the East China Sea shelf with different surface sediment types. Oceanol Limnol Sin 32(1):50–57 (in Chinese)
46. Lim DI, Choi JY, Jung HS, Rho KC, Ahn KS (2007) Recent sediment accumulation and origin of shelf mud deposits in the Yellow and East China Seas. Prog Oceanogr 73:145–159
47. Chen JH, Edwards RL, Wasserburg GJ (1986) ^{238}U, ^{234}U and ^{232}Th in sea water. Earth Planet Sci Lett 80:241–251
48. Wang YH, Jan S, Wang DP (2003) Transports and tidal current estimates in the Taiwan Strait from shipboard ADCP observations (1999–2001). Est Coast Shelf Sci 57:193–199
49. Wu CR, Chao SY, Hsu C (2007) Transient, seasonal and interannual variability of the Taiwan Strait Current. J Oceanogr 63: 821–833
50. Zhao BR, Fang GH (1991) Estimation of water fluxes of major waterways in East China Sea. Acta Oceanol Sin 13(2):169–178 (in Chinese)
51. Kawakami H, Yang YL, Kusakabe M (2009) Distribution of ^{210}Po and ^{210}Pb radioactivity in the intermediate layer of the northwestern North Pacific. J Radioanal Nucl Chem 279:561–566
52. Huh CA, Chen WF, Hsu FH, Su CC, Chiu JK, Lin S, Liu CS, Huang BJ (2010) Modern (<100 years) sedimentation in the Taiwan Strait: rates and source-to-sink pathways elucidated from radionuclides and particle size distribution. Cont Shelf Res 31:47–63